Applying spray pyrolysis to synthesize MnO_x for decomposing isopropyl alcohol in ozone- and thermal-catalytic oxidation

Chung-Liang Chang*, Yu-Chih Lin*,†, Hsunling Bai**, and Yu-Huei Liu**

*Department of Environmental Engineering and Health, Yuanpei University, Hsinchu City, Taiwan
**Institute of Environmental Engineering, National Chiao Tung University, Hsinchu City, Taiwan

Abstract−Manganese oxides (MnO_x) were prepared by spray pyrolysis methods (Mn_S) and calcination at 600 and 1,000 °C (Mn_{600} and Mn_{1000}) in this study. Further, the efficiencies of oxidizing isopropanol (IPA) by these MnO_x utilizing ozone (OZCO) and thermal catalytic oxidation (TCO) were compared. The results indicated that Mn_S, which are characterized by larger surface areas, processed gas hourly space velocity of 42,000 h^{-1} and inlet IPA concentration of 400 ppm performing IPA decomposition efficiencies approaching 100%, and the reaction temperature was operated at only 85 °C for OZCO. The reaction temperature of TCO operated above 270 °C decomposed IPA at the same efficiency.

Key words: Manganese (Mn), Ozone, Volatile Organic Compounds (VOCs), Catalytic Oxidation

INTRODUCTION

Thermal catalytic oxidation (TCO) is a typical technique for removing hazardous pollutants from gas streams, and the catalysts allow oxidation to proceed at lower temperatures compared with thermal oxidation alone [1-3]. Ozone catalytic oxidation requires the addition of ozone to contaminated gas streams before they are passed through a catalyst bed to enable catalytic oxidation reactions [4]. Compared with the operating temperature of TCO, the operating temperature of OZCO can be further reduced, even to room temperature. In addition, adding ozone could enhance the degradation of organic compounds via the photo-catalytic process [5], and OZCO also had good performance on degrading humic acids [6].

Manganese oxides (MnO_x) are considered the most efficient transition-metal catalysts for catalytic oxidation [7,8], and their catalysis for oxidizing acetone, chlorobenzene, toluene, and trichloroethylene has been verified to be excellent at oxidizing temperatures of 300-500 °C [9-14]. OZCO assisted by MnO_x has also been verified to be capable of efficiently oxidizing benzene, toluene, and carbon monoxide (CO) [15]. Further, the oxidizing activity of MnO_x for CO was reported to exceed that of Cr, Fe, Co, and Ni catalysts [16].

Regardless of whether one is concerned with TCO or OZCO, most of the MnO_x is synthesized by calcination with the immersion or sol-gel method. However, the conventional method for manufacturing MnO_x is time consuming, usually requiring more than 32 hours. Recently, novel materials of nano catalysts and adsorbents have been synthesized within a few seconds, respectively, using spray prolysis [17] or aerosol-assisted self-assembly processes [18]. Both the synthesis and processing times of the spray prolysis process are much less than those of the common method for producing catalysts. However, limited information is available in the literature on the applicability of MnO_x synthesized by the spray proly-

sis process as catalysts for TCO and OZCO.

We investigated the oxidation performance of Mn catalysts synthesized by the spray pyrolysis method (Mn_S) for TCO and OZCO. The target pollutant was chosen to be isopropanol (IPA), which is one of the most common VOCs emitted by the semiconductor and optoelectronics industries. The results in terms of different oxidation temperatures and inlet ozone concentrations were also compared with those of a Mn catalyst synthesized by the calcination method at 600 and 1,000 °C (Mn_{600} and Mn_{1000}).

EXPERIMENTS

1. Synthesis

Calcination and spray pyrolysis methods were utilized to prepare different Mn catalytic powders. The calcination catalysts were produced by the procedure of Stobbe et al. [19] and prepared by drying at 105 °C for 24 h with a 0.1 M aqueous solution of $Mn(CH_3COO)_2 \cdot 4H_2O$ (analytical grade, Merck). Then, the MnO_x of the calcination catalysts were calcinated in air at 600 (Mn_{600}) or 1,000 °C (Mn_{1000}) for another 8 h. The spray pyrolysis process of the Mn catalyst (Mn_S) was referred to Kang et al. [17] A 0.1 M aqueous solution of Mn $(CH_3COO)_2 \cdot 4H_2O$ was sprayed at atmosphere pressure with an aerosol atomizer (TSI, Model 3076), yielding an aerosol flow rate of 2.5 LSTP min^{-1}. The aerosol flow passed through a tube reactor (inner diameter: 40 mm) in the two-stage furnace operated at 500 °C and 800 °C, respectively. The length for each stage of the furnace was the same, 600 mm. Then, the aerosol was thermal decomposed and oxidized to form manganese oxide particles.

The specific surface area of the samples was determined by the BET method using nitrogen adsorption-desorption isotherms (Micromeritics ASAP 2020). The crystalline phase of the Mn catalyst was observed by powder x-ray diffraction (XRD, Rigaku D/MAX-B, Japan), and surface observations were obtained by scanning electron microscopy (SEM, HITACHI-S4700).

2. Reactor

The experimental apparatus was composed of three units: a gas-

†To whom correspondence should be addressed.
E-mail: yuchihlin@mail.ypu.edu.tw

eous IPA generation unit, a packed reactor, and a gas analysis unit. A dry-grade compressed gas tank was used for the carrier stream (80% N_2 and 20% O_2). The IPA stream was prepared by purging pre-purified gas through the aeration cylinders. The concentration of IPA was controlled by adjusting either the water bath temperature or the diluting carrier stream. The flow rates of all streams were regulated by mass flow controllers (Brooks, 5850). A dielectric barrier discharge (DBD) system was used to generate ozone [20]. Catalytic reactions were performed in a packed reactor, which contained a thermostat. The diameter of the reactor was 1.3 cm, and the volume of the packing catalysts was 1 cm³.

The experiments were designed to examine the IPA decomposition efficiency catalyzed by MnO_x, which were synthesized by different methods for TCO and OZCO. The baseline operation conditions were as follows: the initial concentration of IPA was 400 ppm and the overall operating flow rate was 700 mL/min (gas hourly space velocity=42,000 h^{-1}). IPA concentrations at the inlet and the outlet of the test reactors were analyzed by gas chromatograph cou-

pled with a flame ionization detector (GC-FID) (China Chromatography 9800) with a packed column (SP-1200, 2-m length). The operation detection limit of GC-FID for the VOCs was 0.5 ppm. Ozone and CO_2 concentrations were analyzed by a Fourier-transformation infrared spectrometer (FTIR, BRUKER, VECTOR 22) equipped with a gas cell (Infrared Analysis, model 2.4-P. A.).

RESULTS AND DISCUSSION

1. Material Analysis

The XRD patterns of the MnO_x are presented in Fig. 1. The crystalline phase of MnO_x presented by the XRD analyses was classified as Mn_3O_4, and those of Mn_{600} and Mn_{1000} were Mn_2O_3 and Mn_3O_4, respectively.

Table 1 illustrates results of the other material analyses of the catalysts. The surface area of Mn_S was 37 m²/g, while those of Mn_{600} and Mn_{1000} were 4.1 and 0.48 m²/g, respectively. The higher calcination temperature of 1,000 °C is thought to result in melting of the structure of Mn_{1000} which decreases the surface area. The apparent densities of Mn_{600} and Mn_{1000} were both about 1 g/cm³; however, that of hollow Mn_S, at 0.37 g/cm³, was less than the others. Fig. 2 shows the effects of the synthesis methods on the appearance of MnO_x as observed on SEM micrographs. The incineration method produced an appearance of Mn_{600} of pieces and pillared granules; however, due to the high temperature and instantaneous time of the spray pyrolysis method, which enhances quick-drying of the surface of Mn precursor droplets in the synthesis procedure, the Mn_S product displayed pearls, rings, and hollow particles. These forms also improved the surface area of Mn_S over that of Mn_{600}. The results indicated the surface area of MnO_x was lower during calcina-
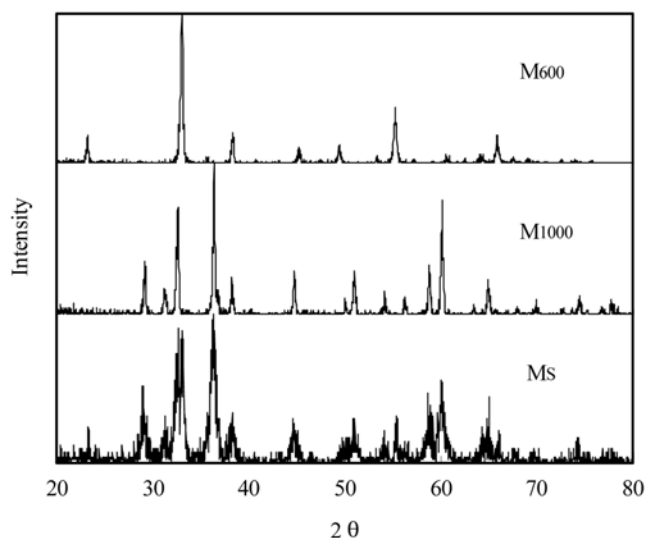

Fig. 1. X-ray diffraction (XRD) pattern of manganese oxides (MnO_x).

Table 1. Material analysis of the adsorbents

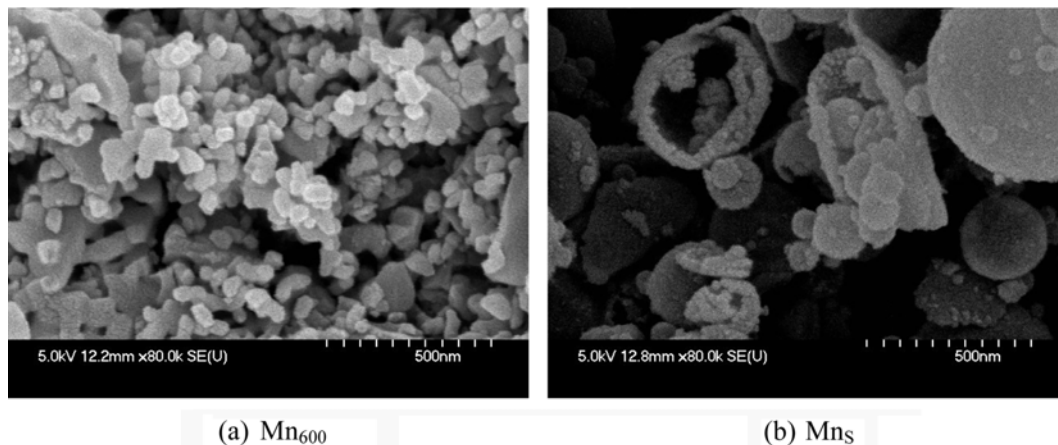| Catalyst	Crystalline phase	Surface area (m²/g)	Apparent density (g/cm³)
Mn_{600}	Mn_2O_3	4.1	0.91
Mn_{1000}	Mn_3O_4	0.48	1.24
Mn_S	Mn_3O_4	37.0	0.37

(a) Mn_{600}

(b) Mn_S

Fig. 2. Scanning electron microscopic (SEM) images of manganese oxides (MnO_x) synthesized by (a) calcination at 600 °C and (b) by spray pyrolysis.

tion method. The conventional MnO$_x$ catalysts are prepared via a precipitation method from Mn(NO$_3$)$_2$ with carbonates and hydroxides to obtain the higher surface area [21]. However, the precipitation method was a complex procedure, including adjusting pH of precursor, washing, filtering, drying, and calcinations. Compared with the precipitation method, spray pyrolysis is a direct method to obtain MnO$_x$ catalysts characterized as higher surface area.

2. Thermal Catalytic Oxidation (TCO)

In the TCO experiments, Fig. 3 shows the effects of reaction temperatures between 130 and 360 °C on the decomposition efficiencies of IPA with TCO. At the lower temperature of 130 °C, the Mn$_S$ could process IPA at a decomposition efficiency of 41%, but the decomposition efficiencies of Mn$_{600}$ and Mn$_{1000}$ were <10%. All decom-

position efficiencies of MnO$_x$ were enhanced with increasing reaction temperatures. When the temperature reached 250 °C, both Mn$_S$ and Mn$_{1000}$ showed decomposition efficiencies of >97%; however, Mn$_{600}$ showed the same efficiency when operated at >320 °C.

When MnO$_x$ were operated at reaction temperatures of <177.5 °C, the selectivity of IPA conversion to acetone was > 80%, and this selectivity decreased with rising reaction temperatures. The selectivities of acetone and CO$_2$ were calculated as:

$$S_{acetone} = \frac{[\text{concentration of acetone}] \times 3}{[\text{total reacted concentration of carbon}]} \times 100\% \qquad (1)$$

$$S_{CO_2} = \frac{[\text{concentration of CO}_2]}{[\text{total reacted concentration of carbon}]} \times 100\% \qquad (2)$$

(a) Mn$_{600}$
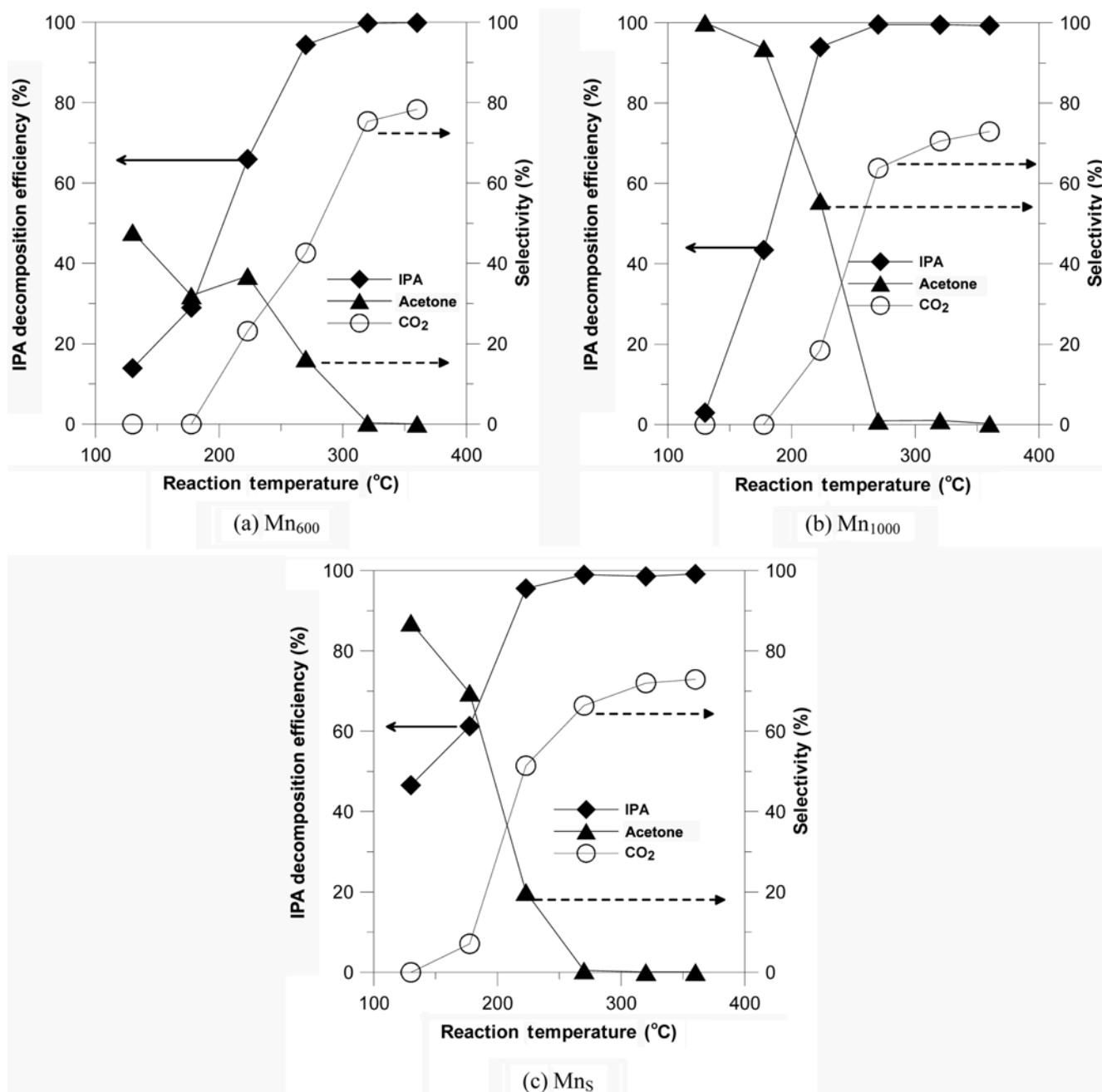
(b) Mn$_{1000}$

(c) Mn$_S$

Fig. 3. Effects of reaction temperatures on the decomposition efficiency of isopropanol (IPA) in thermal catalytic oxidation (TCO).
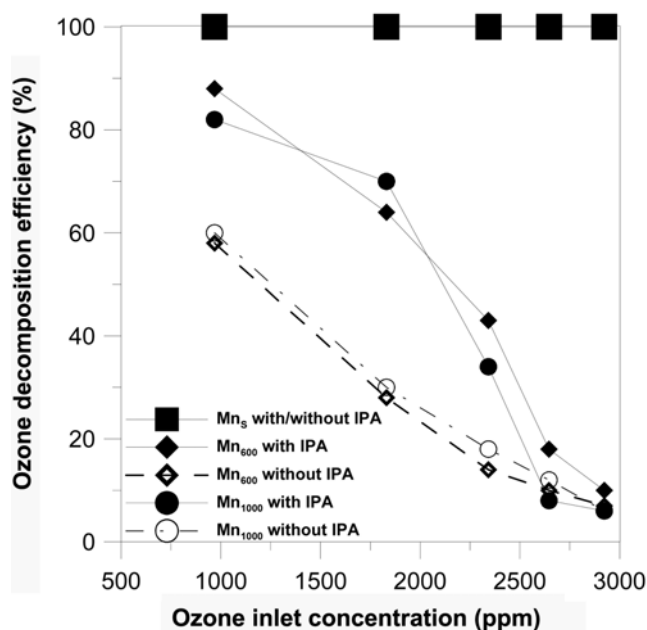
Fig. 4. Effects of the different manganese oxides (MnO_x) and the presence of isopropanol (IPA) on the ozone decomposition efficiencies.

The total reacted concentration of carbon was defined as:

$$\text{total reacted concentration of carbon} = [IPA]_{in} - [IPA]_{out}. \quad (3)$$

Fig. 3 also indicates that MnO_x operated above 270 °C enhanced the efficiency of IPA oxidization to CO_2, but decreased the selectivity to acetone. When the reaction temperature rose to 360 °C, the efficiency of IPA oxidization to CO_2, which was catalyzed by Mn_{600}, Mn_{1000}, and Mn_S, respectively increased to 79%, 68%, and 73%. The above results corresponded to those of Gil et al. [22], who indicated that the performance of catalysts with Mn_2O_3 crystals in the complete oxidation of acetone was superior to that with Mn_3O_4 crystals. The superior performance was attributed to the crystalline structure of Mn_2O_3, but the MnO_x with larger surface areas did not exhibit a higher ratio for the complete oxidation of acetone. Thus, the reaction rate for TCO was governed by diffusion in the crystalline structure, but not the reaction on the surface area.

3. Ozone Catalytic Oxidation (OZCO)

Fig. 4 shows a comparison of the ozone decomposition efficiencies among Mn_S, Mn_{600}, and Mn_{1000}, at the reaction temperature of 85 °C with and without the presence of IPA. When the ozone concentration was increased from 910 to 2,900 ppm, the decomposition efficiencies of the Mn_S negligibly differed, and a decomposition efficiency of 100% was maintained. In contrast, the efficiency of other MnO_x decreased with increasing ozone concentrations. When the ozone concentration was 910 ppm, both Mn_{600} and Mn_{1000} processed ozone with a decomposition efficiency of only 59% in the absence of IPA. When processing the higher ozone concentration, the efficiency of Mn_{600} was close to that of Mn_{1000}. The principal factor affecting the efficiency of ozone decomposition by MnO_x was the surface area in this study.

The higher surface area of the Mn catalyst enhanced the efficiency, and resulted in an ozone processing efficiency of Mn_S being supe-

rior to that of Mn_{600} and Mn_{1000}. This was because the OZCO mechanism is a surface reaction; however, the different crystalline phases produced insufficient effects on the ozone decomposition efficiency.

Fig. 4 also indicates the effect of the presence of IPA on the ozone decomposition efficiency, which enhanced the ozone decomposition efficiency of MnO_x. This is because ozone on the surface of MnO_x was decomposed to oxygen radicals and oxygen, and the oxygen radicals reacted with IPA to reduce the amount. Thus, ozone decomposition was accelerated based on the stoichiometry of the overall reaction, thereby improving the decomposition efficiency.

The efficiencies of MnO_x in the OZCO decomposition of IPA are illustrated in Fig. 5. The results show that all MnO_x had excellent performance efficiencies in decomposing IPA at the lower temperature. In other words, ozone enhanced the performance of the catalyst in oxidizing IPA. Mn_S exhibited the best performance of oxidizing IPA among all of the tested catalysts, and the efficiencies were in the decreasing order of Mn_{1000} and Mn_{600}. Fig. 5 also indicates the effect of ozone concentration on the selectivity of IPA conversion to acetone. When the ozone concentration in the OZCO was 970 ppm, the selectivities catalyzed by Mn_{600}, Mn_{1000}, and Mn_S were 85%, 84%, and 60%, respectively.

In addition, the IPA decomposition efficiencies of Mn_{600}, Mn_{1000}, and Mn_S catalyst were 8.7%, 8.78%, and 17%. When the ozone concentration rose to 2,700 ppm, the IPA decomposition efficiencies of Mn_{600}, Mn_{1000}, and Mn_S also respectively improved to 26%, 38%, and 75%. Further, Mn_S could completely decompose IPA to CO_2 at an ozone concentration of 3,300 ppm, even at the lower temperature of 85 °C, but TCO did not have sufficient efficiency at that lower temperature. However, comparing the results in Figs. 3 and 5, the intermediate amount of acetone in TCO at the higher temperature was less than that in OZCO, and CO_2 production in TCO was more than that in OZCO.

The sum of selectivity for each product does not correspond to 100% for all experimental data, which indicates that some intermediates existed in the reaction due to the incomplete mineralization of IPA. Carbon monoxide was presumed appearing in outgas, because CO was one of intermediates in the dielectric barrier discharge (non-thermal plasma) system for VOCs abatement [23,24]. In addition, Wu et al. [25] indicated that some intermediates of IPA oxidation in ozone-based advanced oxidation processes included acetic acid, formic acid, and oxalic acid. Therefore, the results in this study indicate that a higher temperature and more ozone are necessary for complete oxidation.

CONCLUSIONS

The Mn_S catalyst with OZCO and a proper ozone concentration processed gas hourly space velocity of 42,000 h^{-1} and inlet IPA concentration of 400 ppm performing IPA decomposition efficiencies approaching 100% at only 85 °C, and produced no residual ozone; in addition, the decomposition efficiency of IPA decomposed by Mn_S was nearly 100%, but the temperature of TCO had to be raised to 270 °C. The ratio of complete oxidization with TCO at the higher temperature was superior to that with OZCO.

In addition, Mn_S utilized in the OZCO and TCO showed excellent performance in the decomposition efficiency of IPA. Mn_S manufactured by spray prolysis not only had a better performance, but
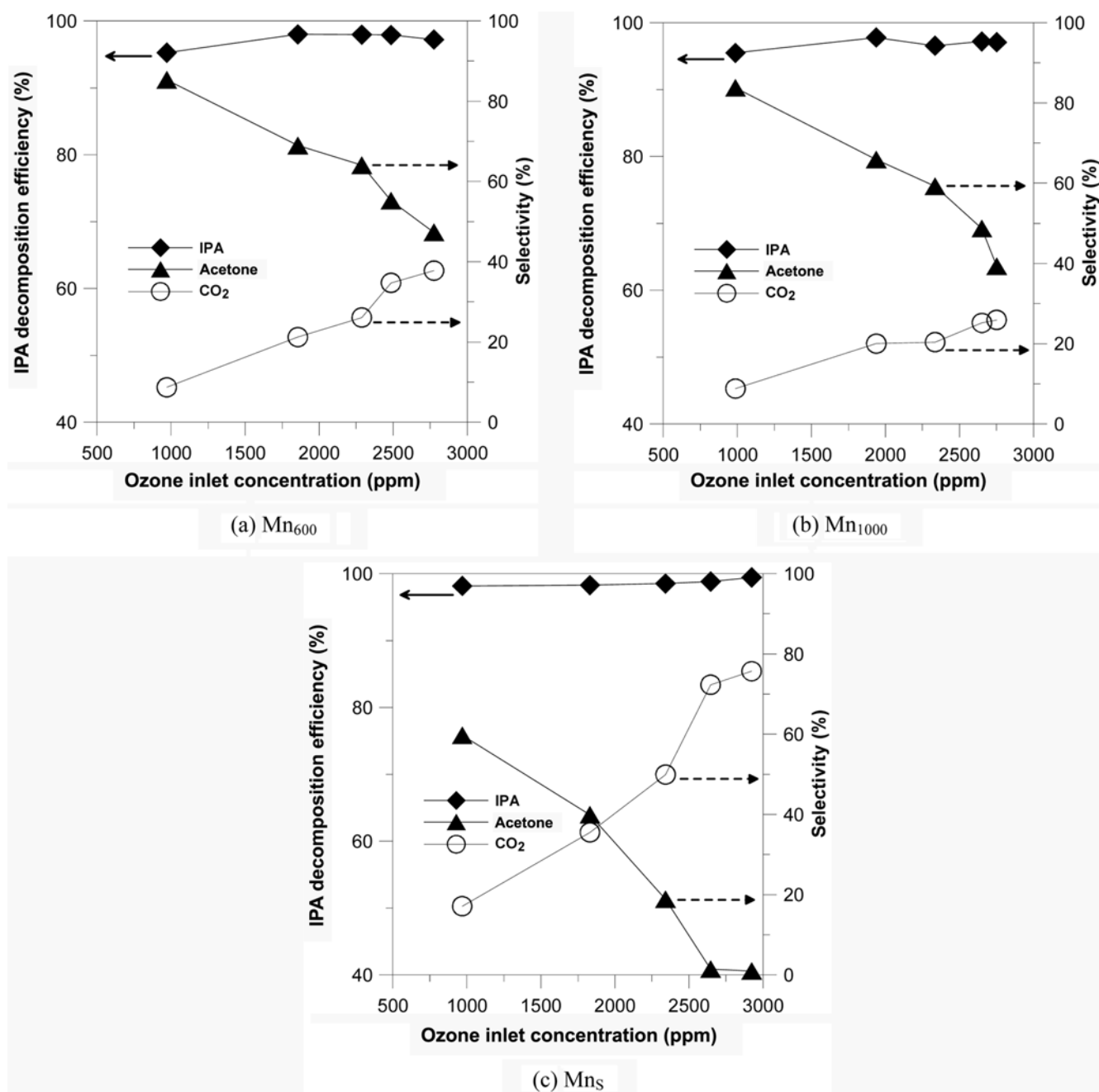
Fig. 5. Effects of ozone concentration on the decomposition efficiency of isopropanol (IPA) in ozone catalytic oxidation (OZCO).

the synthesis and processing times of the spray prolysis process were less than those of the common method for producing catalysts.

REFERENCES

1. B.-H. Jang, S.-S. Lee, T.-H. Yeon and J.-E. Yie, *Korean J. Chem. Eng.*, **15**, 516 (1998).
2. J. Kirchnerová, *Korean J. Chem. Eng.*, **16**, 427 (1999).
3. S.-S. Hong, G.-H. Lee and G.-D. Lee, *Korean J. Chem. Eng.*, **20**, 440 (2003).
4. D. Mehandjiev, A. Naydenov and G. Ivanov, *Appl. Catal. A: Gen.*, **206**, 13 (2001).
5. S.-J. Yoa, Y.-S. Cho and J.-H. Kim, *Korean J. Chem. Eng.*, **22**, 364 (2005).
6. J.-E. Lee, B.-S. Jin, S.-H. Cho, S.-H. Han, O.-S. Joo and K.-D. Jung, *Korean J. Chem. Eng.*, **22**, 536 (2005).
7. P. Ciambelli, S. Cimino, S. De Rossi, M. Faticanti, L. Lisi, G. Minelli, I. Pettiti, P. Porta, G. Russo and M. Turco, *Appl. Catal. B: Environ.*, **24**, 243 (2000).
8. M. Baldi, E. Finocchio, F. Milella and G. Busca, *Appl. Catal. B: Environ.*, **16**, 43 (1998).

9. L. M. Gandia, M. A. Vicente and A. Gil, *Appl. Catal. B: Environ.*, **38**, 295 (2002).

10. A. Gil, L. M. Gandia and S. A. Korili, *Appl. Catal. A: Gen.*, **274**, 229 (2004).

11. Y. Liu, M. Luo, Z. Wei, Q. Xin, P. Ying and C. Li, *Appl. Catal. B: Environ.*, **29**, 61 (2001).

12. T. K. Tseng, H. Chu and H. H. Hsu, *Environ. Sci. Technol.*, **37**, 171 (2003).

13. D. Dobber, D. KieBling, W. Schmitz and G. Wendt, *Appl. Catal. B: Environ.*, **52**, 135 (2004).

14. B. Nowicki, J. Hetper and Z. Wietrzynska-Lalak, *React. Kinet. Catal. Lett.*, **75**, 323 (2002).

15. B. Dhandapani and S. T. Oyama, *Appl. Catal. B: Environ.*, **11**, 129 (1997).

16. Y. A. Aleksandrov, I. A. Vorozheikin, K. E. Ivanovskaya and E. I. Tsyganova, *Russ. J. Gen. Chem.*, **71**, 825 (2001).

17. Y. C. Kang, S. B. Park and Y. W. Kang, *NanoStruct. Mat.*, **5**, 777 (1995).

18. Y. Lin, H. Bai and C. Chang, *J. Air Waste Manage. Assoc.*, **55**, 834 (2005).

19. E. R. Stobbe, B. A. de Boer and J. W. Geus, *Catal. Today*, **47**, 61 (1999).

20. C. L. Chang and T. S. Lin, *React. Kinet. Catal. Lett.*, **86**, 91 (2005).

21. M. Kang, E.-D. Park, J.-M. Kim and J.-E. Yie, *Appl. Catal. A: Gen.*, **327**, 261 (2007).

22. A. Gil, L. M. Gandia and S. A. Korili, *Appl. Catal. A: Gen.*, **274**, 229 (2004).

23. S. L. Brock, T. Shimojo, S. L. Suib, Y. Hayashi and H. Matsumoto, *Research on Chemical Intermediates*, **28**, 13 (2002).

24. M. Magureanu, N. B. Mandache, V. I. Parvulescu, C. Subrahman-yam, A. Renken and L. Kiwi-Minsker, *Appl. Catal. B: Environ.*, **74**, 270 (2007).

25. J. J. Wu, J. S. Yang, M. Muruganandham and C. C. Wu, *Sep. Purif. Technol.*, **62**, 39 (2008).